

Article

# Dynamics of Land Use and Land Cover Changes in Harare, Zimbabwe: A Case Study on the Linkage between Drivers and the Axis of Urban Expansion

Andrew K. Maroneddze \* and Brigitta Schütt \*

Department of Earth Sciences, Physical Geography, Freie Universität Berlin, Malteserstr. 74-100, Haus H, 12249 Berlin, Germany

\* Correspondence: ak.maroneddze@fu-berlin.de (A.K.M.); brigitta.schuettt@fu-berlin.de (B.S.);  
Tel.: +49-30-838-70239 (A.K.M. & B.S.)

Received: 9 September 2019; Accepted: 16 October 2019; Published: 19 October 2019



**Abstract:** With increasing population growth, the Harare Metropolitan Province has experienced accelerated land use and land cover (LULC) changes, influencing the city's growth. This study aims to assess spatiotemporal urban LULC changes, the axis, and patterns of growth as well as drivers influencing urban growth over the past three decades in the Harare Metropolitan Province. The analysis was based on remotely sensed Landsat Thematic Mapper and Operational Land Imager data from 1984–2018, GIS application, and binary logistic regression. Supervised image classification using support vector machines was performed on Landsat 5 TM and Landsat 8 OLI data combined with the soil adjusted vegetation index, enhanced built-up and bareness index and modified difference water index. Statistical modelling was performed using binary logistic regression to identify the influence of the slope and the distance proximity characters as independent variables on urban growth. The overall mapping accuracy for all time periods was over 85%. Built-up areas extended from 279.5 km<sup>2</sup> (1984) to 445 km<sup>2</sup> (2018) with high-density residential areas growing dramatically from 51.2 km<sup>2</sup> (1984) to 218.4 km<sup>2</sup> (2018). The results suggest that urban growth was influenced mainly by the presence and density of road networks.

**Keywords:** urban growth; built-up area; Harare Metropolitan Province; binary logistic regression; support vector machines

## 1. Introduction

Temporally and spatially, urbanization is an uneven process supporting residential expansion, including growth in population size of individuals living in urban areas and expansion of physical structures in an urban setup in addition to the previously existing structures [1,2]. Urbanization is directly changing and affecting the environment, as it is made distinct by the increasing built-up and impervious areas at the expense of wetland areas and agricultural landscapes. Such actions result in the transformation of natural landscapes into agricultural landscapes [3]. Consequently, this leads to environmental degradation through deterioration of vegetation and sealing, often resulting in increasing surface runoff, soil erosion, surface water contamination, and exploitation of natural habitats [4–6]. Muller et al. [7] highlights that urbanization is one of the greatest factors contributing to biodiversity loss due to the expansion of industrial, residential and commercial business areas.

The world's population is projected to increase from 7.0 to 9.3 billion by 2050 [8]. Therefore, during that stipulated period urban areas worldwide are anticipated to absorb large numbers of the growing population. Urbanization is a continuous process, and megacities such as Delhi, India had a total increase in population of 47.02% within a decade between 1991 and 2001 [9]. For China, the

urbanization growth rate tripled from 17.9% to 57.4% between 1978 and 2016, and it is projected to reach 70% by 2035 [10]. Although countries like Ethiopia are among the least urbanized countries in the world, high rates of in-migration to urban cities have been investigated and projected to reach 42.1% of the total population by 2050 [11]. Up-to-date data and information regarding the trends and status of urban ecosystems are required to enable the development of sustainable strategies on improving livelihoods in urban settings. In particular, in sub-Saharan Africa, up-to-date data and information on population are fundamental for developing ways to curb urban demographic transitions [12]. It is estimated that sub-Saharan Africa's urban population will rise by 60–70% by 2050, with most people occupying small cities due to the fact of cultural, socio-economic and political influences [12,13]. Although previous studies have indicated urban growth in terms of population size, studies on land use and land cover (LULC) changes and the key drivers of such changes remain scarce yet important.

To further understand the relationship between urbanization and environmental alteration, LULC changes need to be assessed and evaluated to determine the extent and the rate at which human activities are contributing to shifts in the environment. The integration of remote sensing data to monitor the state and dynamics of the Earth's surface provides reasonable results in a short space of time [6], compared to on-site surveying techniques [14,15]. Moderate resolution Landsat Thematic Mapper images (TM) are a standard tool used for urban mapping and change detection analysis and were used, for example in Minnesota, USA between 1986 and 2002 for LULC changes [16]. Landsat images in combination with socio-economic data have been used to determine the effects associated with development and land use shifts. For example, spatial dynamics of LULC changes were analysed for the Nairobi urban area and showed that the built-up area quadrupled from 1.9% in 1976 to 8.6% of the total area in 2000 [17]. For Zimbabwe, Hove and Tirimboi [18] indicated that on a national scale, vast numbers of people migrated to Harare from rural homes soon after independence in 1980. Wania et al. [19] reported on the expansion of built-up areas of Harare using high-resolution SPOT images.

Investigation of LULC change dynamics and classification in heterogeneous landscapes using moderate-resolution satellite imagery potentially has challenges due to the fact of spectral confusion resulting in misleading information [20,21]. Accurate observation of LULC changes by remote sensing is a vital component of promoting sustainability. Enhancement of land cover class delineation using remote sensing indices and machine learning algorithms such as random forest (RF) and support vector machines (SVMs) have the relatively desirable characteristic of improving multispectral classification [20–24]. The effectiveness of mapping land-cover types using spectral indices is primarily the result of their ability to characterize relative features of interest over a wide range of the spectrum [25]. The Harare Metropolitan Province was chosen as a case study because of its vastly reported pressures due to the presence of high population and urbanization rates for this metropolitan area in the northern High Veldt of Southern Africa [19,26]. Harare Metropolitan Province, being the capital city of Zimbabwe, faces increasing population growth as do other metropolitan cities largely because they are associated with better livelihoods and as centres for economic activities, public services, and amenities [24,27]. Among others, Chirisa and Muhomba [28] revealed that Epworth, a Harare Metropolitan Province district, has approximately 70% of its inhabitants living on unauthorized, non-serviced land and thereby compounding the increased settlement and spread of the metropolitan area. Thus far, monitoring urban growth trends is an important tool for understanding previous trends and present growth patterns and potentially unravelling possible coming developments and their likely impacts [29]. Identifying empirical drivers of urban structure change is based on past and current state of LULC changes for the Harare Metropolitan Province. The current study aimed to investigate the axis of change and expansion of the Harare Metropolitan Province. In view of the resource constraints in a developing country, freely available remote sensing data were applied to assess the direction of the urban expansion. Furthermore, the study sought to determine the explanatory drivers of the changes in LULC for the Harare Metropolitan Province.

## 2. Materials and Methods

### 2.1. Study Area

The study area lies between  $17^{\circ}49'39.79''$  south latitude and  $31^{\circ}03'12.13''$  east longitude and covers three districts of the Harare Metropolitan Province (Figure 1) [26,30]. Harare is the capital city of Zimbabwe and experiences high urbanization rates from rural–urban shifts, driven by those in search of better livelihoods and employment [31,32]. The bedrock in Harare Metropolitan Province are granites in the east and southwest and gabbro and dolerite in the north, while phyllite and metagreywacke dominate the core centre of the Harare Metropolitan Province [26,33,34]. The relief is slightly rolling with locally U-shaped incised valleys. Bedrock is widely covered by several decimetre-thick saprolite which is characterized by cyclic surface erosion that exposes bedrock [35].

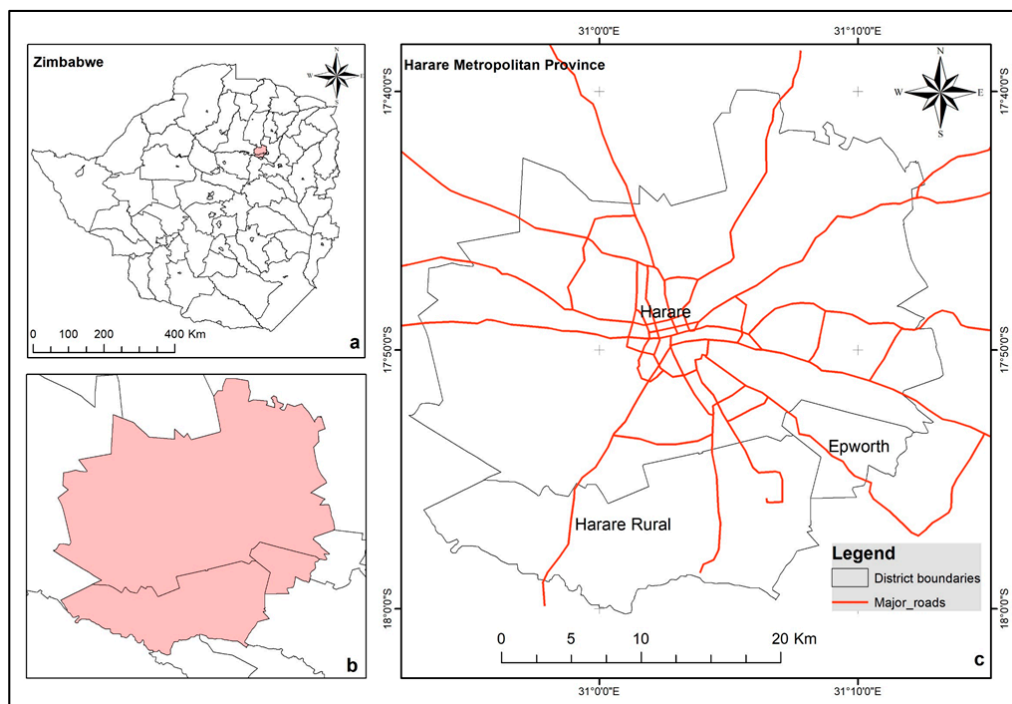


**Figure 1.** Location of the Harare Metropolitan Province composed of the Harare urban, Harare rural, and Epworth districts. (a) Zimbabwe district boundaries highlighting the study area; (b) Harare Metropolitan Province study boundaries; (c) major roads marked in the Harare Metropolitan Province map indicating the major urbanisation axis.

The climate is sub-tropical with four seasons: a cool–dry season from mid-May to August; a hot–dry season from September to mid-November; a rain–wet season from mid-November to mid-March; and a post rainy season stretching from mid-March to mid-May [26,30]. During the cold–dry season, temperatures range from  $7^{\circ}\text{C}$  to  $20^{\circ}\text{C}$ , while during the hot–dry, season temperatures range from  $13^{\circ}\text{C}$  to  $28^{\circ}\text{C}$ . On average, the Harare Metropolitan Province receives annually 470 mm to 1350 mm of rainfall, most of it during rainy season [26]. In the Harare Metropolitan Province, the Harare urban district was estimated to have a population of 1,435,784 in 2002 and 1,485,231 in 2012; for the Harare rural district, a population of 23,023 in 2002 and 113,599 in 2012; and for the Epworth district, a total population of 114,047 in 2002 and 167,462 in 2012 [36,37]. The total area of the Harare Province, in which the study area was embedded, extends over  $940\text{ km}^2$  [19].

### 2.2. Data Acquisition and Pre-Processing

Cloud-free Landsat satellite images of  $30\text{ m} \times 30\text{ m}$  resolution were acquired from the United States Global Survey (USGS; [www.earthexplorer.usgs.gov](http://www.earthexplorer.usgs.gov)). These Landsat satellite images were selected

because of their adequacy and availability for LULC classification, as indicated by multiple studies (among others, [16,38]). Landsat 5 Thematic Mapper images were selected for the years 1984, 1990, 2000, 2008 and Landsat 8-OLI image for the year 2018 (Table 1).

**Table 1.** The Data used for land use and land cover (LULC) classification and their date of acquisition.

Sensor	Number of Bands	Path/Row	Date of Acquisition
Landsat 5 TM	7	172/072	22 June 1984
Landsat 5 TM	7	172/072	23 June 1990
Landsat 5 TM	7	172/072	30 August 2000
Landsat 5 TM	7	172/072	11 August 2008
Landsat 8 OLI	11	172/072	11 August 2018

All satellite images were acquired for the cool–dry season with completely clear (0%) cloud-free coverage. All satellite images were geometrically corrected using topographic sheets at 1:50,000 and applying 20 ground control points collected using a handheld GPS (Garmin 60Cx) at major road intersections. First-order polynomial transformation was used for the retrieved satellite image scenes and the obtained root mean square errors (RMSEs) were less than half the pixel dimensions. A projected vector map for Harare Province was used to clip the study area from the pre-processed images for classification and modelling. Images provided by the USGS were already corrected for radiometric distortions. Resampling was done using the nearest-neighbourhood technique in order to retain the original pixel values. The QGIS 3.4 software was applied to further correct atmospheric distortions and conversion of digital numbers (DNs) to spectral reflectance through dark object subtraction [39]. Prior conversion of DN to reflectance urban indices were computed using RStoolbox, a package in R, and then further computation of vegetation indices.

### 2.3. Field Data Collection and Processing

During field observations in December 2018, the LULC class structure (Table 2) was determined. Field data were collected, recording randomly 600 land cover sample points using a handheld GPS (Garmin 60Cx). The points were randomly split into two sets: 80% of the data for training and 20% of the data for accuracy assessment and validation [30]. Polygons (regions of interest (ROIs)) were digitized and used for both LULC classification and accuracy assessment to improve classification and validation range [23].

**Table 2.** Description of the study LULC classes.

ID	LULC Class	Description
1	CBD/industries	Industries and central business district defined with a high fraction of impervious surfaces, mainly buildings and a small proportion of vegetation
2	LMD residential	Leafy and well-established low- and medium-density suburbs surrounded with high vegetation
3	HD residential	High-density residential areas with low vegetation cover or clustered settlements with areas undergoing developments and bare exposed land
4	Irrigated cropland	Cultivated land under irrigation schemes
5	Rain-fed cropland	Cultivated land or land with crop residues after harvesting
6	Vegetation	All wooded areas, shrubs and bushes, riverine vegetation and grass covered areas
7	Water	Areas occupied by water, rivers, wetlands, reservoirs and dams

CBD: central business district; LMD: low to medium density; HD: high density.

Statistical testing of spectral separability of the desired classes was verified using the transformed divergence separability index (TD) to ensure classification [40]. Figure 2 documents the approach and flow path used in the study. Topographic maps, expert knowledge and auxiliary data were used to create ground truth areas of interest for Landsat images from 1984, 1990, 2000 and 2008 for classification and accuracy assessment. Field observations and ground control points (GCPs) were obtained for 2018 time slices.

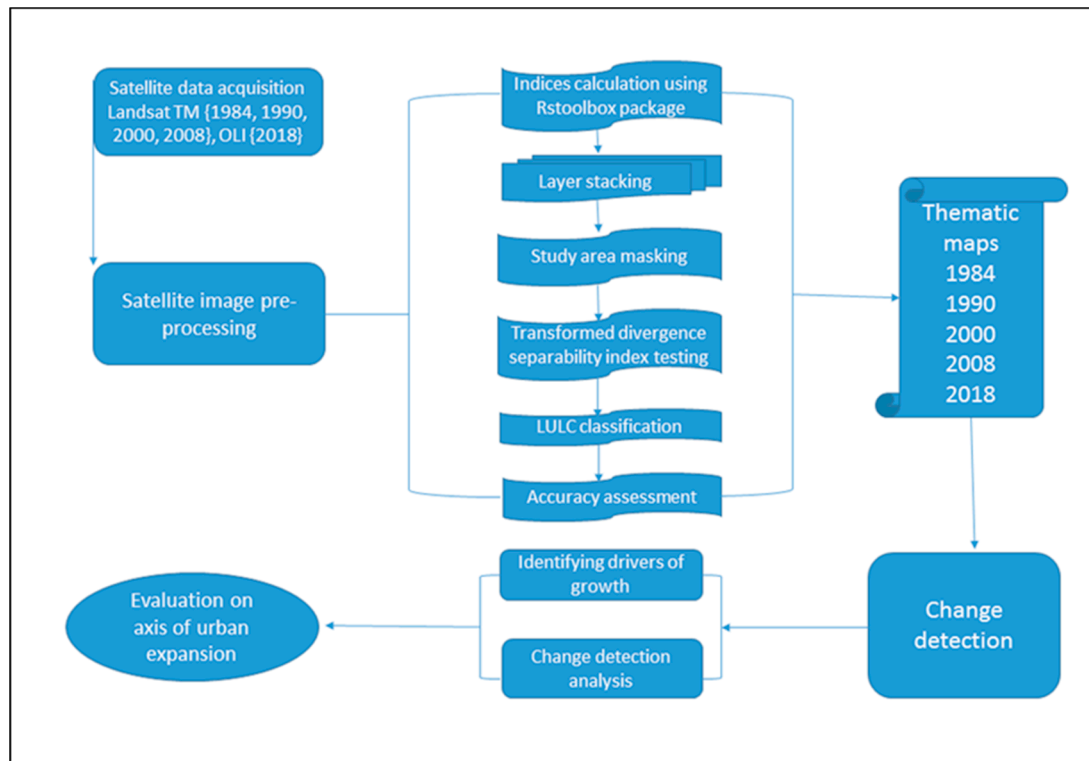


**Figure 2.** Flowchart showing the determination of drivers and the axis of urban expansion for Harare Metropolitan Province.

#### 2.4. Land Cover Classification

The LULC maps were created for the years 1984, 1990, 2000, 2008 and 2018 using supervised support vector machine (SVM) algorithms on 30 m band stacks for each image scene and an additional three layers applying different indices: enhanced built-up and bareness index (EBBI), modified normalized difference water index (MNDWI) and soil adjusted vegetation index (SAVI) for all stacks. These additional band stacks enhanced the mapping of the major urban LULC cover classes, namely, built-up, open water body and vegetation [24,41]. Support vector machines correspond to machine learning classification methods which have a high ability to minimise misclassification errors by reducing the probability of misclassifying field data collected having an unknown probability distribution [42]. Each image was classified into seven classes that were determined by spectral characterization and field data substantiated training and accuracy assessment.

An accuracy assessment was computed for the Kappa coefficient (Kc), overall accuracy (OA), producer's accuracy (PA) and user's accuracy (UA), applying "ground truth regions of interests" [23,43]. Accuracy assessment is a probabilistic approach that computes the association between remotely sensed and referenced data. Post classification change detection matrices were cross-tabulated in ENVI using five interval steps: 1984–1990, 1990–2000, 2000–2008, 2008–2018 and 1984–2018. The post classification change detection method involved pixel-by-pixel change analysis highlighting spatio-temporal LULC changes and distribution.



### 2.5. Computation of Spectral Indices

Enhancing spectral signals of overbuilt areas, vegetation and water in remotely sensed data was done through computation of multiple spectral bands [24]. The enhanced built-up and bareness index (EBBI), modified normalized difference water index (MNDWI) [44] and soil adjusted vegetation index (SAVI) were selected to improve the extraction of major land-use classes in a heterogeneous urban built-up area. The EBBI allows mapping of built-up and bare areas using a combination of near infrared (NIR), short wave infrared (SWIR) and thermal infrared (TIR) on which these bands were selected according to the contrast reflection and absorption in bare and built-up areas [21].

$$EBBI = \frac{SWIR1 - NIR}{10 \sqrt{SWIR1 + TIRS1}} \quad (1)$$

The SAVI requires soil-brightness correction factor  $L$ , which varies from 0 for very high vegetation cover to 1 for very low vegetation cover; a 0.5 soil-brightness correction factor  $L$  was used because of its moderate [45].

$$SAVI = \frac{(NIR - R)}{(NIR + R + L)} \times (1 + L), 0 < 1 < 1 \quad (2)$$

The MNDWI uses SWIR in enhancing open water extraction in a complex heterogeneous setup because of the high reflectance obtained in built-up areas to the spectral band. Henceforth, negative values for built-up areas and positive values for water features makes the MNDWI suitable for discriminating built-up areas from water features [24,44].

$$MNDWI = \frac{GREEN - SWIR}{GREEN + SWIR} \quad (3)$$

### 2.6. Binomial Logistic Regression

A binomial logistic regression was applied to analyse the explanatory drivers of LULC changes. The form variable slope ( $^{\circ}$ ) was used as a topographic factor, while the proximity characters factored in included distance to the main roads, distance to secondary roads, distance to open water bodies, distance to streams and distance from the city centre [41–43]. For the binomial regression, the growth variables (dichotomous dependant) applied were raster layers with transformed cells from any LULC to built-up area between 1984 and 2018 (Figure A1). Proximity and topographic characters formed the basis of the independent variables (distance to the main roads, distance to secondary roads, distance to open water bodies, distance to streams and distance from the city centre). Distances were calculated using the Euclidean distance tool in ArcGIS 10.2 to determine the impact of urban expansion relating to the proximity of the selected features encompassing the road network for transportation and water courses as environmental amenities.

The cell values of the dependant variable (dichotomous raster layer) which had been changed from any other LULC class to an urban built-up area for all time steps (i.e., 1984–1990, 1990–2000, 2000–2008, 2008–2018, 1984–2018) were set to be urban growth (=1), while all cells which did not change to an urban built-up area or had been an urban built-up area previously were set as non-urban growth (=0) using the raster calculator in ArcGIS 10.2. A total of 7000 stratified random sample points were created to extract cell values from the LULC maps of all time slices for regression analysis and available sets of data. A collection of 6139 random sample points was assembled, and the remaining outliers were removed because they were scattered outside of the rasters. Extracted distance proximity parameter values were log-transformed and, during computation, a 30 m value equivalent to cell length was added to all cells in order to counter undefined 0 logarithm for predictors applied in the regression analysis [46]. The statistical significance of  $p < 0.05$  indicated that the relation between predictor and LULC change occurrences were not random, highlighting a statistical relation between the independent proximity variable and an urban built-up area. The evaluation of model performance was calculated using statistical measures of the discriminatory effect of the model, the area under

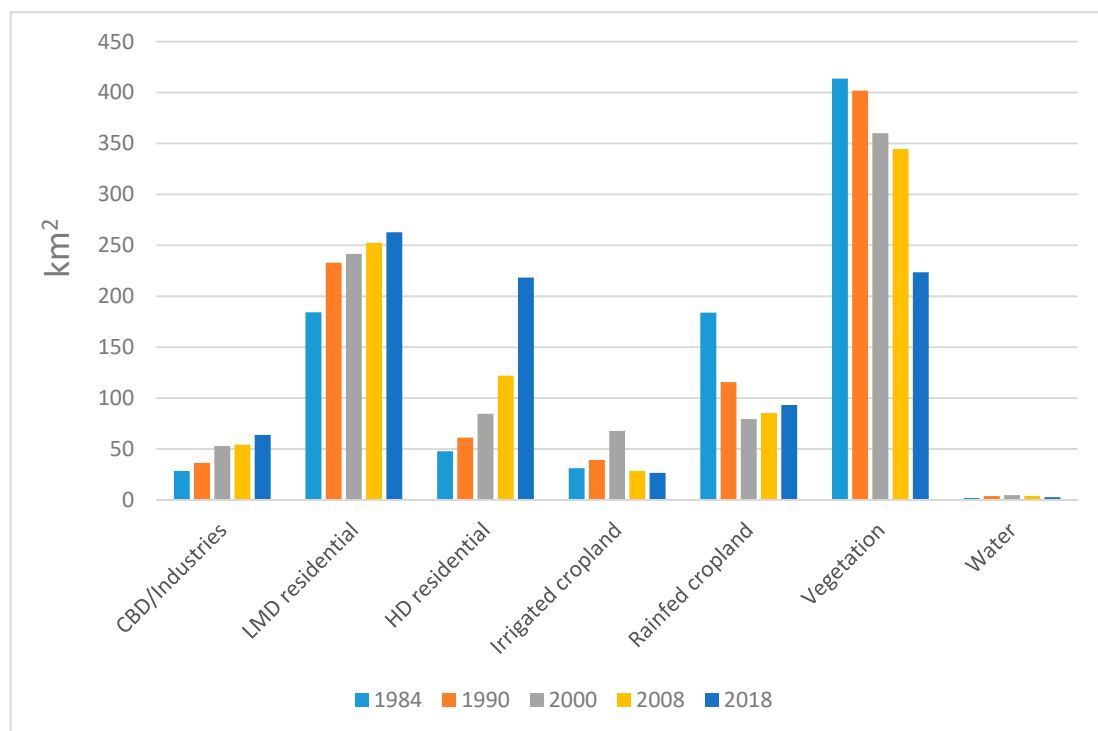
the receiver–operating–characteristic (ROC) curve (AUC) and the percentage of correct predictions (PCPs) [47–49].

Data for location characterization was retrieved from various sources. Open water and streams data were digitized from topographic maps [47]; trunk and secondary roads were extracted from OpenStreetMap data (OSM-Geofabric [48]); and the digital elevation model (DEM) of the Shuttle Radar Topography Mission (SRTM) with a 30 m resolution was accessed from United States Geological Survey website (<https://earthexplorer.usgs.gov/>). Each data set was normalized into ranges from 0–1 using the min–max linear transformation by applying the raster calculator (Map Algebra) in ArcGIS so that all input data used the same range [49].

### 3. Results

#### 3.1. Area Extent and Change of Land Use and Land Cover

The data revealed an increase in the high-density residential areas and, consequently, a decrease in the area covered by vegetation all over the Harare Metropolitan Province (Figure 3, Figure 4, Table 3). In the year 1984, high-density residential areas covered 51.79 km<sup>2</sup> (5.81%) of the total Harare Metropolitan Province, while, by the year 2018, it had more than quadrupled reaching 218.35 km<sup>2</sup> covering almost a quarter of the Harare Metropolitan Province area. The data also showed a steady increase in central business department (CBD) or industrial areas from 3.7% in 1984 to 7.17% in 2018. In addition, coverage by low- to medium-density suburb areas steadily increased, covering 21.85% of the Harare Metropolitan Province in 1984 to 29.48% in 2018. Apparently, in 1984, vegetation covered almost half of the area (448.67 km<sup>2</sup>) of the total Harare Metropolitan Province but decreased by nearly 50% to 223.45 km<sup>2</sup> (25.08%) by the year 2018 (Figure 3, Figure 4, Table 3).



CBD: central business district; LMD: low to medium density; HD: high density.

**Figure 3.** Area sizes showing changes in the LULC classes in the Harare Metropolitan Province.

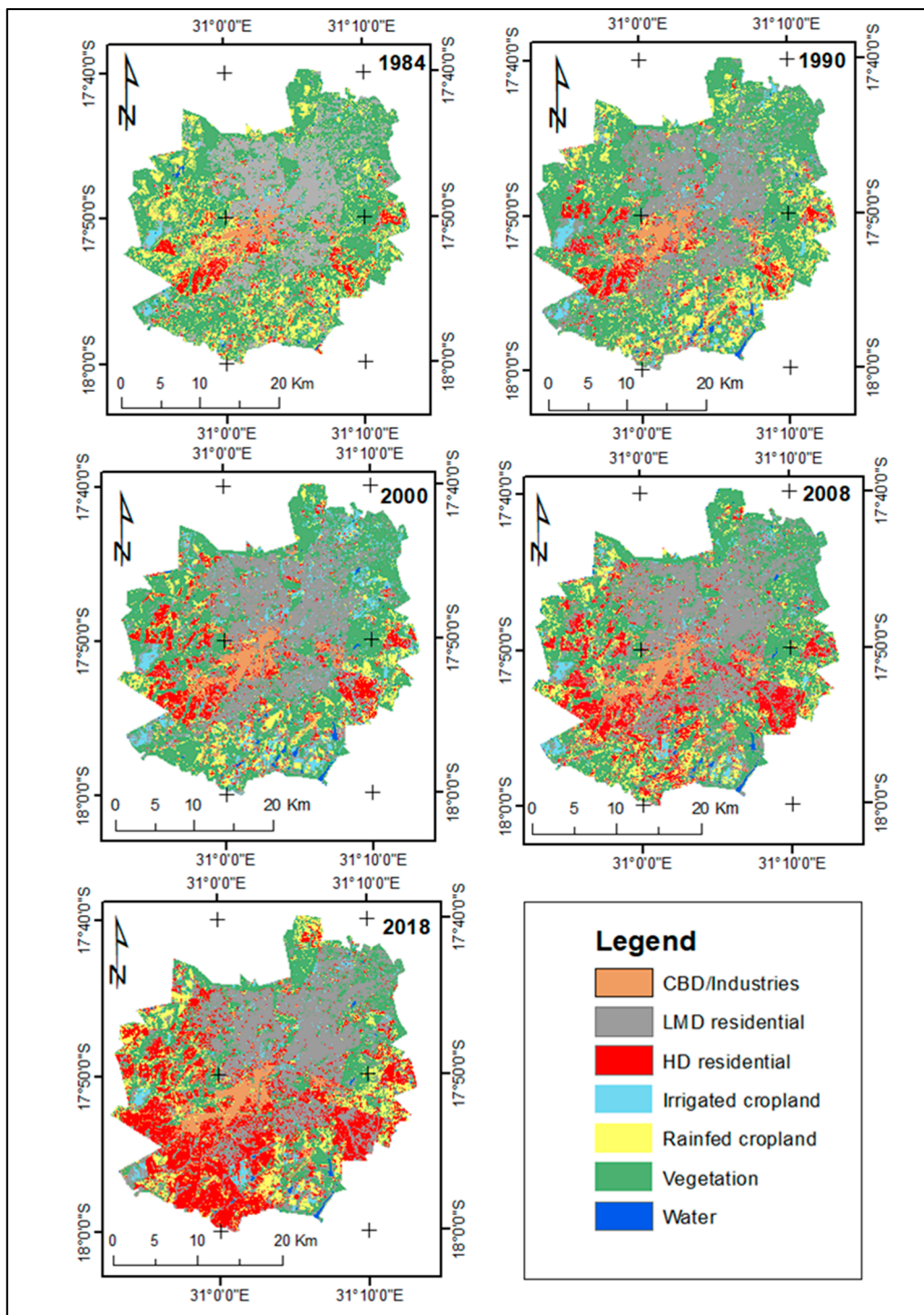


**Figure 4.** Land use and land cover in the Harare Metropolitan Province for the years 1984, 1990, 2000, 2008 and 2018.

The spread of croplands (combined irrigated and rain-fed croplands) decreased from a coverage of 17.89% of the Harare Metropolitan Province in 1984 to 13.40% in 2018. The areas covered by water slightly increased from about 0.40% in 1984 to 0.53% in 2000; however, this coverage declined sharply to 0.31% in 2018. Between 1984 and 1990, high-density residential areas were spreading towards the west and northwest of the city (Figure 4). Yet, between 1990 and 2018, a spread of urbanized areas can be seen towards the south, southwest, and southeast of the Harare Metropolitan Province (Figure 4). In



addition, low- to medium-density suburbs expanded towards the northeast of the Harare Metropolitan Province, increasing from 21.85% in 1984 to almost 30% of the area in 2018 (Figure 4; Table 3).

**Table 3.** Net change of the LULC by class area extent (km<sup>2</sup>) and percentage (%) of the Harare Metropolitan Province.

LULC Class	1984		1990		2000		2008		2018	
	km <sup>2</sup>	%	km <sup>2</sup>	%	km <sup>2</sup>	%	km <sup>2</sup>	%	km <sup>2</sup>	%
CBD/industries	32.95	3.70	36.27	4.07	52.98	5.95	54.27	6.09	63.88	7.17
LMD residential	194.72	21.85	233.02	26.15	241.53	27.11	252.48	28.33	262.74	29.48
HD residential	51.79	5.81	61.13	6.86	84.61	9.49	121.96	13.69	218.35	24.50
Irrigated cropland	18.13	2.04	39.30	4.41	67.77	7.61	28.55	3.20	26.68	2.99
Rainfed cropland	141.26	15.85	115.74	12.99	79.34	8.90	85.42	9.59	93.26	10.47
Vegetation	448.67	50.35	401.88	45.10	360.13	40.41	344.48	38.66	223.45	25.08
Water	3.60	0.40	3.78	0.42	4.76	0.53	3.96	0.44	2.76	0.31

CBD: central business district; LMD: low to medium density; HD: high density.

### 3.2. Land Use and Land Cover Classification Accuracy

For each time slice 1984, 1990, 2000, 2008 and 2018, each LULC class was compared to the reference data for classification accuracy assessment. The overall accuracy (OA) of the LULC classification varied for the different time slices between 85%–90% (1984: 90.1%, 1990: 85.1%, 2000: 88.9%, 2008: 87.6%, 2018: 89.7%; Table 4). The high separability indices produced were due to the enhancing effects from the vegetation and enhanced built-up and bareness indices incorporated and displayed improved mapping accuracy (Table S1). The transformed divergence separability index (TD) indicates that if values are greater than 1.9, separability among classes will be very high showing that classes are separable, while values smaller than 1.0 are deemed not statistically separable for good classification [33]. The highest misclassifications were recorded for the LULC classes, such as high-density residential areas (all time slices), irrigated cropland, and rain-fed cropland (1990), as indicated by the producer's accuracy (Table 4, Table A1, Table A2).

**Table 4.** Land use and land cover classification accuracies in percentages for the study period 1984–2018. The accuracies include Kappa coefficient (Kc), overall accuracy (OA), producer's accuracy (PA) and user's accuracy (UA).

LULC Class	1984		1990		2000		2008		2018	
	PA	UA	PA	UA	PA	UA	PA	UA	PA	UA
CBD/industries	94.7	93.7	99.2	93.7	96.7	90.3	96.4	96.4	96.6	95.3
LMD residential	89.4	90.2	81.9	87.3	87.4	92.4	84.5	75.5	84.1	84.6
HD residential	82.2	85.0	77.7	93.3	83.4	89.9	79.8	83.5	92.9	92.5
Irrigated cropland	87.6	95.1	78.4	91.9	76.2	82.3	93.0	87.4	84.4	83.3
Rain-fed cropland	84.1	87.2	67.4	80.5	85.6	79.0	90.9	79.6	86.8	88.7
Vegetation	93.4	90.1	92.9	71.1	90.2	82.4	79.1	91.8	88.9	88.9
Water	89.3	96.9	98.4	100	97.3	99.5	98.9	99.8	99.2	100
OA	90.1		85.1		88.9		87.6		89.7	
K <sub>C</sub>	0.87		0.82		0.86		0.85		0.87	

CBD: central business district; LMD: low to medium density; HD: high density.

### 3.3. Binomial Logistic Regression

The value of the area under the receiver–operating–characteristic (ROC) curve (AUC) shows the discriminatory effect of the model and statistically validates the predictive urban growth drivers' behaviour [45]. The predictive effect of the AUC ranges from 0.5 to 1, where 0.5 shows a completely random relationship and 1 shows that the model has a perfect discriminatory effect. The true positive

rate (TPR) is the proportion of cells which are correctly classified and the false positive rate (FPR) is the proportion of incorrectly classified cells by the real urban growth occurrences [44,45]. The percentage of correct predictions (PCPs) shows the percentage of correctly predicted points from the total number of available points [47,50]. The PCPs range from 0 to 1, where values greater than 0.5 (50%) indicate that the model predicts the outcome better than PCP closer to 0 [47].

Between 1984 and 1990, the AUC amounted to 0.679 (Figure 5) and, according to the regression coefficients, a significant influence from the nearest distance to major and secondary roads was only revealed among all other test predictors. The  $p$ -values for the predictors distance to the city centre, distance to the stream, distance to open water, and for variable slope were not significant ( $p > 0.05$ ), suggesting that they had no influence on the growth and spread of the urban built-up area. Between 1990 and 2000, the model reveals that the distance to major and secondary roads and the city centre were significant variables ( $p < 0.05$ ) influencing the urban built-up area expansion with a discriminatory AUC value of 0.669 (Figure 5). Between 2000 and 2008, the predictors nearest distance to major and secondary roads, distance to the city centre and distance to open water and slope were significant ( $p < 0.05$ ) in the binomial logistic regression model showing that they had influence on urban built-up area expansion with an overall AUC value of 0.683 (Figure 5).

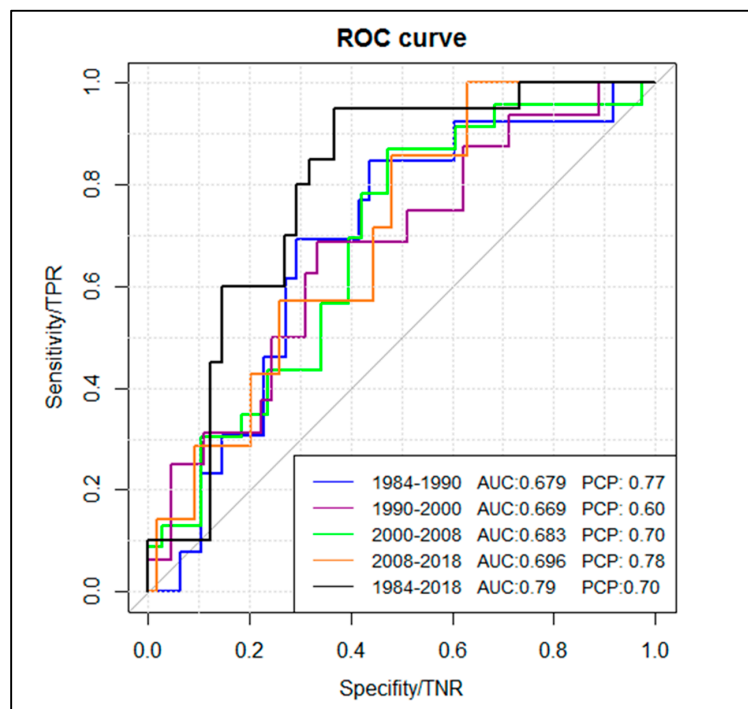


**Figure 5.** Receiver–operating–characteristic (ROC) curves conveying binomial logistic regression analyses results for urban growth from 1984 to 2018 within the Harare Metropolitan Province (TPRs: true positive rates; TNRs: true negative rates; AUC: area under the curve; PCPs: percentage of correct predictions).

Distance to the nearest roads, distance to the nearest streams, open water and slope were statistically significant as predictors of the urban built-up area expansion and spread ( $p < 0.05$ ) between 2008 and 2018, with an AUC value of 0.696 (Figure 5). The nearest distance to the city centre predictor was not significant ( $p > 0.05$ ). From 1984 to 2018, distance to the nearest major and secondary roads, streams, open water and slope were significant predictors to explain the urban built-up area expansion with an AUC value of 0.79 (Figure 5). The influence of the distance to the city centre as a predictor for urban built-up area expansion decreased due to the increasing outward expansion and spread of the Harare Metropolitan Province towards its peripheries.

#### 4. Discussion

Urbanization has modified the Harare Metropolitan Province through the expansion of built-up areas at the expense of vegetation, cropland and water bodies (Figures 3 and 4). Similarly, urbanization processes investigated in Daqahlia, a city in Egypt, depicted that the built-up area expanded from 4.2% of the area under investigation in 1985 to 36.3% in 2010, while areas used as cropland shrank by 30.7% and areas covered by water decreased by 0.45% [27]. An increase of 219.5% in LULC change, mainly attributed to land development at the expense of cropland, fallow land, water, shrub and bare land, was revealed in the Shanghai metropolis between 1997 and 2008 showing the impact of land use change and population growth in urban areas [51]. Akure city in the southwest of Nigeria experienced a similar loss of areas covered by vegetation and water bodies as the Harare Metropolitan Province due to the fact of built-up area expansion, from 5.1% in 1986 to 53.41% in 2014 for the total area under investigation [6].

In the current study, a SVM classification method was applied because it potentially produces better accuracy in a confusion matrix compared to other neural networks, maximum likelihood and decision trees when mapping LULC [50,51]. However, possible sources of error in the calculations may have emerged from geometric rectification, accuracy in digitizing topographic maps and combining different data sources. The spectral differences and characteristics between Landsat 5 TM and Landsat 8 OLI sensors may have affected the accuracy of the thematic maps [23]. Despite these potential discrepancies, the classification and results obtained in the current study have relatively high accuracy considering urban area spectral heterogeneity characteristics and spectral confusion from land cover classes, and the results agree with other published scientific studies carried out at the national and regional level (Supplementary Materials Table S1) [6,24,26,27]. The use of hyper-spectral data and aggregation of urban built-up areas have been observed to improve and enhance the analysis of remote sensing data in urban areas [50,52]. The utilization of additional built-up, water and vegetation remote sensing indices bands on the Landsat imagery scenes provide a substantial improvement in the mapping of an urban area using moderate-resolution imagery [21,44,45]. However, misclassifications and reduction of areas covered by water bodies (water class) might have resulted from the increasing density of water hyacinths along the streams due to the fact of contaminated sewage effluents deposited in the water ecosystem [52,53]. This is directly linked to the inflow of effluents from industries, sewage disposal (punctual sources) and urban agriculture (diffuse sources). Consequently, alteration of water bodies as aquatic weeds scattering on the surfaces potentially influences classification (Table 4).

The current study looked at the axis of urban development and the drivers posing LULC changes. This study revealed that the distance to the nearest major and secondary roads have a large impact on urban expansion and development. The binary logistic regressions highlight that built-up area development occurred predominantly along the major roads and in dense road network areas (i.e., secondary roads), due to the high connectivity and easy access to transport facilities. Hegazy and Kaloop [27] reiterate that urban growth follows development along highways or already established cities as a result of population growth and socioeconomic factors. Nevertheless, high-density residential areas are expanding towards the periphery of the south, southeast, southwest and northwest of Harare Metropolitan Province. For comparison, the results of modelling the distance characters in Bucharest were in line with the findings of the current study—major and secondary roads impact positively on urban growth and expansion of built-up areas [53]. For Bucharest, however, independent variables such as distance to lakes and rivers were not significant, while for the Harare Metropolitan Province, these variables have significant influence, as revealed by the binomial regression analysis between 2008 and 2018. Henceforth, the exclusion of the core city of Bucharest from the Bucharest Metropolitan area could have reduced the ability of the model to detect some independent characters. Still the geographic location of the study areas, socioeconomic structure and population sizes are highly different.

The current study reveals that zones of urban area or built-up area expansion were associated with relatively gentle undulating slopes (Figure S1) which can be attributed to low housing costs, cheap land acquired through housing schemes and informal urban settlements [19]. The southwest

part of the Harare Metropolitan Province was the main direction of urban spread between 1984 and 1990 (Figure A1). This was associated with the expansion from first old Harare high-density suburbs that were designated during the colonial period such as Highfields, Mufakose and Rugare, among others [54]. These areas are associated with high-density road networks, low costs and economic residential units compared to the low and medium density residential areas. Between 1990 and 2000, expansion of the Harare Metropolitan Province dominated much in the southwest, west and southeast (Figure 4, Figure A1). This expansion can be attributed to urban sprawling and rampant informal settling due to the presence of socio-economic factors in the eastern direction—that is, the Epworth suburbs and Dzivarasekwa extension introduced in 1991 [55,56]. Between 2000 and 2008, significant expansion of built-up areas was directed towards the south and northwest direction (Figure 4, Figure A1) regardless of “Operation Murambatsvina” (Restore Order), a clean-up campaign that was carried out in June 2005 and left Harare with dismal identifiable illegal, urban built-up structures [31].

The expansion of Harare Metropolitan Province between 2008 and 2018 was dominant in the southern direction, and the city was expanding towards its peripheries (Figure 4, Figure A1). The far continued expansion towards the southeast resulted from unplanned urban development because of population pressure [28]. Bureaucracy and rigid and stringent procedures relating to construction plans approval by local authorities posed a hindrance towards sustainable urban growth [57–59]. Fast urban built-up area growth was observed on the southeast parts of Harare [19] resulting in marginalized urban residents. These marginalized urban residents are residing in poorly serviced areas which are of relatively low cost due to the shunning absence of proper water and sewer reticulation systems. This unplanned development accompanied with poor sanitary conditions resulted in increased chances of severe health issues [60,61].

The northeast of Harare Metropolitan Province is composed of low-density residential suburbs and is characterized by medium gradient hills covered by high-vegetation density compared to high-density residential suburbs (Figure 4) [34,54]. Due to the stratification of Harare, high income earners were pronounced to occupy these vegetation-enriched suburbs [55]. Construction on these landscapes is costly resulting in the variable “slope” as a significant driver for urban-built up area growth since the larger proportion of Harare residents occupied flat to gentle undulating landscapes in the south and other parts of Harare (Figure 4, Figure S1). Urban built-up area expansion towards the high-density residential area in the northwest direction follows the establishment of housing schemes such as the University of Zimbabwe’s Association of University project and Hatcliffe Consortium development [31,59]. The Hatcliffe Consortium development was a government initiative on Operation “Garikai/Hlalani kuhle” projects meant to provide housing units towards the “Operation Murambatsvina” victims [31]. On the other hand, high population density on the northwest suburbs of Harare coincides with increasing urban built-up area expansion [19,30].

The geometry of road network reveals an influence on the spatial distribution and spread of urban built-up area as characterized by the regression models capturing the changes between 1984 and 2018 (Figure 5). This indicates a linear pattern on the built-up areas and the road network systems, contributing to the rapid spreading of informal settlements within the road spheres. Easy access to transportation network systems paves the way for a linear and grid distribution pattern of built-up areas in urban cities such as the Harare Metropolitan Province. The urban population increased faster than anticipated, resulting in accelerated rates of informal settlements and the erratic provision of decent housing by the Zimbabwean Government [28,58,62]. Increased unrestrained built-up area expansion and spread in the south and east of the Harare Metropolitan Province reveals largely urban sprawl [26,28]. Thus, these increasing rates of informal settlements within the metropolitan area have negatively impacted water resources. Thereby, driving the “distance to the nearest streams and open water” variables as influential characters of the urban built-up area expansion. This has also been attributed to the invasion of the Harare Metropolitan Province’s ecosystem with urban construction activities [26,37,59]. The outward spreading of built-up areas was not evenly distributed. It concentrated largely in the south and southeast parts of the Harare Metropolitan Province, where

fairly flat landscapes occur. This contributes to cheap residential construction costs [19] compared to the strongly rolling, sloppy landscape in the northeastern suburbs of the Harare Metropolitan Province (Figure 4, Figure A1) [34].

Without negating population growth rate as a driving force for urban growth, there is a correlation between urban expansion and population growth rate as substantiated by previous Harare Metropolitan Province population statistics [29]. The Harare Metropolitan Province population is estimated to have increased from approximately 830,000 in 1982 [28] to 2,098,199 in 2012 [29]. This huge growth of urban population posed large threats to water bodies (open water and streams) thereby making water resources vulnerable. Consequently, urban sprawl and unplanned rampant settling in the Harare Metropolitan Province concurred with the deterioration of water bodies since 2000. Overall, this study indicates that the popularity of water resources as amenities for land estates declined due to urban growth which has led to the degradation of water resources through various human activities.

## 5. Conclusions

This study investigated the influence of independent variables as urban growth explanatory characters using binary logistic regression. The LULC classification accuracy of the Harare Metropolitan Province was improved through the use of remote sensing indices for spectral separability considering the heterogeneity of an urban area. There are fundamental changes observed in the urban built-up area expansion and spread over the past three decades as evidenced by the shrinking of vegetation, cropland and water classes. This burdens the environment due to the increased demand for land by processes such as unplanned urban sprawl and informal settlements. However, there is need for a multi-disciplinary approach including land suitability analysis in order to curb the deterioration of these scarce and fragile resources. Models indicate that growth has been driven by the distance to nearest major roads, secondary roads, streams, open water courses and slope. For the phase between 1984 and 2000, binary logistic regressions show that distance to the city centre and distance to the nearest secondary roads and major roads were significant variables for urban built-up area expansion and spread. We observed a decreasing influence of the distance to the city centre as a predictor for urban built-up area expansion with increasing outward urban spread towards its peripheries. The findings revealed that fast urban growth and built-up area expansion were concentrated largely in the low-lying southern parts of the Harare Metropolitan Region and were occupied by high-density suburbs compared to the slow development in the strongly rolling, sloppy landscapes in the northeast of Harare Metropolitan Province with low-density suburbs. Overall, the model indicates that a road network has greater impact on the development of urban built-up area due to the accessibility of a transport network for connectivity and showing potential areas for future development.

Moreover, the research findings provide a guiding approach for town planners and policy makers to respond and pay attention to Harare Metropolitan Province landscapes which are profoundly deteriorating and, furthermore, the need to conserve the remaining amenities to maintain ecosystem balance.

**Supplementary Materials:** The following are available online at <http://www.mdpi.com/2073-445X/8/10/155/s1>, Figure S1: Overview of slope across the Harare Metropolitan Province derived from a 30 m digital elevation model, SRTM-1ARC (USGS, 2014); Table S1: Transformed divergences indices showing interclass separability of land use and land cover classes used for training and accuracy assessment (CBD: central business district, LMD: low to medium density, HD: high density).

**Author Contributions:** Conceptualization, Methodology, Software, Validation, Formal Analysis, Investigation, Resources, Data Curation, Visualization, Writing—Original Draft Preparation, A.K.M.; Writing—Review and Editing, B.S.; Supervision, B.S.; Project Administration, Funding Acquisition, A.K.M. and B.S.

**Funding:** We thank the German Academic Exchange Service (DAAD) who provided a fellowship to conduct this study. We also acknowledge the financial support by the German Research Foundation and the Open Access Publication Fund of the Freie Universität Berlin.

**Acknowledgments:** The publication of this article was funded by Freie Universität Berlin. We thank our colleagues from Freie Universität Berlin, who provided valuable insights and expertise that greatly assisted this study. We are



grateful to the National Aeronautics and Space Administration (NASA) and the United States Geological Survey (USGS), for providing the high-resolution satellite images and the one Arc-Second Global data from the Shuttle Radar Topography Mission (SRTM) for providing terrain corrected data.

**Conflicts of Interest:** The authors declare no conflict of interest. The funders had no role in the design of the study; in the collection, analyses, or interpretation of data; in the writing of the manuscript, or in the decision to publish the results.

## Appendix A

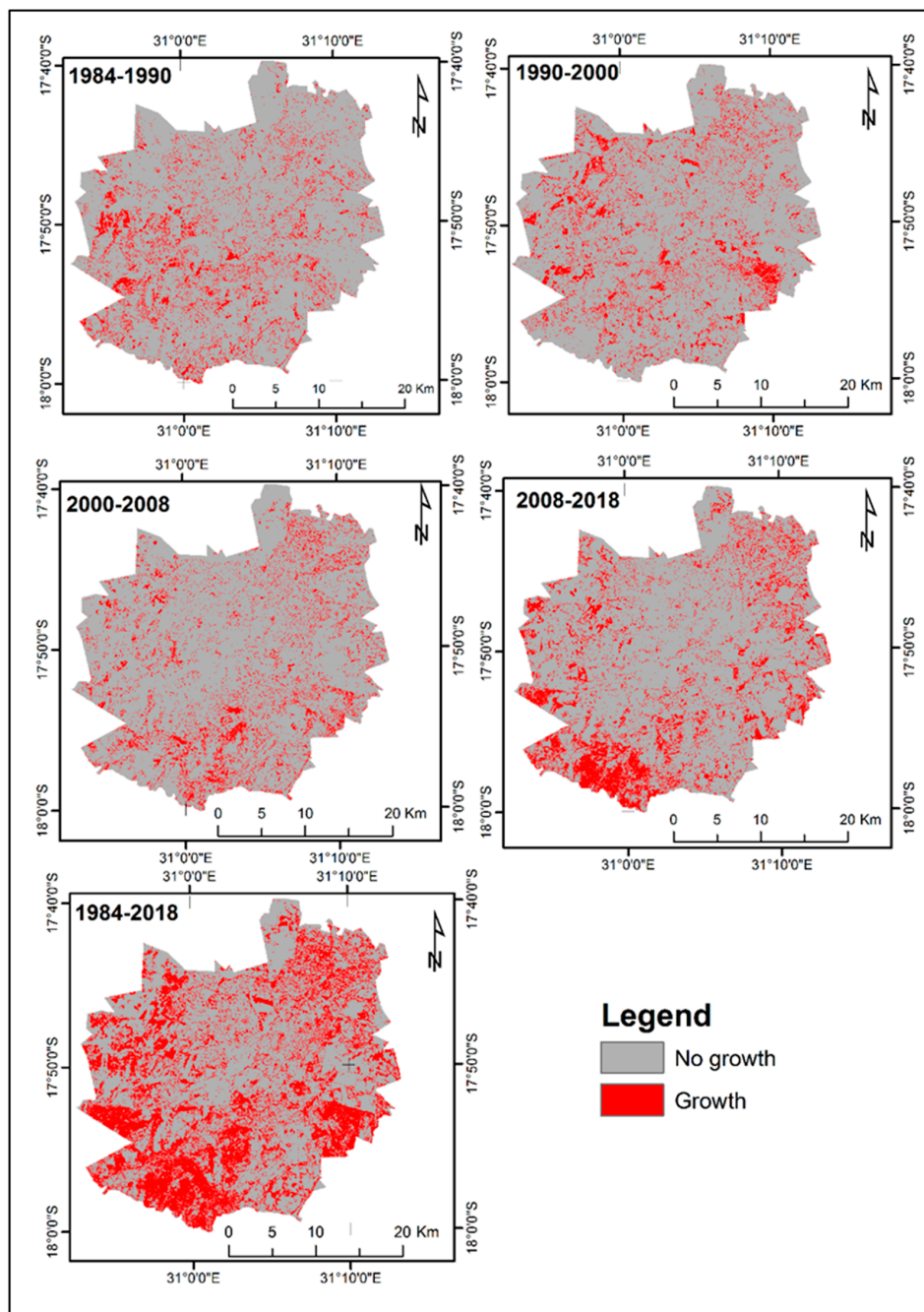


**Figure A1.** Raster layers for dependant variables for all time slices derived from change detection: 1984–1990; 1990–2000; 2000–2008; 2008–2018 and 1984–2018 with urban built-up area growth (=1) and non-built-up area (=0).

**Table A1.** Confusion matrix and associated classification accuracies produced from Landsat 5 TM (1984, 1990, 2000 and 2008). These include kappa coefficient (Kc), overall accuracy (OA), producer's accuracy (PA) and user's accuracy (UA).

1984 Landsat 5 TM		Reference Class								
Classified	Class	CBD/Industries	LMD	HD	Irrigated cropland	Rainfed cropland	Vegetation	Water	Total	PA
	CBD/Industries	4012	182	81	0	3	2	2	4282	94.7
	LMD	92	9353	164	213	8	495	47	10,372	89.4
	HD	98	105	2005	0	135	17	0	2360	82.2
	Irrigated cropland	0	108	2	2602	1	22	0	2735	87.6
	Rainfed cropland	19	37	165	7	5996	655	0	6879	84.1
	Vegetation	10	665	23	148	987	16,765	11	18,609	93.4
	Water	7	9	0	0	0	0	500	516	89.3
	Total	4238	10,459	2440	2970	7130	17,956	560	45,753	
	UA	93.7	90.2	85.0	95.1	87.2	90.1	96.9		
	OA	90.1				Kc	0.87			
1990 Landsat 5 TM		Reference Class								
Classified	Class	CBD/Industries	LMD	HD	Irrigated cropland	Rainfed cropland	Vegetation	Water	Total	PA
	CBD/Industries	1827	62	61	0	0	0	0	1950	99.2
	LMD	1	2335	127	137	0	64	10	2674	81.9
	HD	10	55	979	4	1	0	0	1049	77.7
	Irrigated cropland	0	45	40	1030	6	0	0	1121	78.4
	Rainfed cropland	2	56	45	29	964	102	0	1198	67.4
	Vegetation	2	299	8	114	459	2172	0	3054	92.6
	Water	0	0	0	0	0	0	601	601	98.4
	Total	1842	2852	1260	1314	1430	2338	611	11,647	
	UA	93.7	87.3	93.3	91.9	80.5	71.1	100		
	OA	85.1				Kc	0.82			

Table A1. Cont.

2000 Landsat 5 TM					Reference Class					
	Class	CBD/Industries	LMD	HD	Irrigated cropland	Rainfed cropland	Vegetation	Water	Total	PA
Classified	CBD/Industries	1946	113	85	1	8	3	0	2156	96.7
	LMD	10	3225	30	47	8	157	14	3491	87.4
	HD	50	34	1053	35	0	0	0	1172	83.4
	Irrigated cropland	0	70	53	596	0	5	0	724	76.2
	Rainfed cropland	5	24	38	93	602	0	0	762	85.6
	Vegetation	1	220	3	10	85	1520	6	1845	90.2
	Water	0	3	0	0	1	1	728	732	97.3
	Total	2012	3689	1262	782	703	1686	748		
	UA	90.3	92.4	89.9	82.3	79.0	82.4	99.5		
OA	88.9				Kc	0.86				
2008 Landsat 5 TM					Reference Class					
	Class	CBD/Industries	LMD	HD	Irrigated cropland	Rainfed cropland	Vegetation	Water	Total	PA
Classified	CBD/Industries	2217	21	61	0	0	0	0	2299	96.4
	LMD	15	1629	116	37	0	355	6	2158	84.5
	HD	37	76	746	12	15	8	0	894	79.8
	Irrigated cropland	0	87	2	647	0	4	0	740	93.0
	Rainfed cropland	6	11	3	0	666	151	0	837	90.9
	Vegetation	11	105	7	0	52	1961	1	2137	79.1
	Water	1	0	0	0	0	0	606	607	98.9
	Total	2287	1929	935	695	733	2479	613	9672	
	UA	96.4	75.5	83.5	87.4	79.6	91.8	99.8		
OA	87.6				Kc	0.85				

CBD: central business district; LMD: low to medium density; HD: high density.

**Table A2.** Confusion matrix and associated classification accuracies produced from Landsat 8 OLI (2018). The accuracies include kappa (Kc), overall accuracy (OA), producer’s accuracy (PA) and user’s accuracy (UA).

2018 Landsat 8 OLI		Reference Class								
	Class	CBD/Industries	LMD	HD	Irrigated cropland	Rainfed cropland	Vegetation	Water	Total	PA
Classified	CBD/Industries	2492	63	60	0	1	0	0	2616	96.6
	LMD	23	2721	59	124	64	219	5	3215	84.1
	HD	43	86	1778	10	3	3	0	1923	92.9
	Irrigated cropland	1	134	3	806	0	24	0	968	84.4
	Rainfed cropland	18	7	11	15	1352	122	0	1525	86.8
	Vegetation	4	223	3	0	137	2942	0	3309	88.9
	Water	0	0	0	0	0	0	601	601	99.2
	Total	2581	3234	1914	955	1557	3310	606	14,157	
	UA	95.3	84.6	92.5	83.3	88.7	88.9	100		
OA	89.7				Kc	0.87				

CBD: central business district; LMD: low to medium density; HD: high density.

## References

1. Samson, K. Squatter settlement and the issue of regulation: A case of Dire Dawa. *Ethiop. Local Gov. Dev. J.* **2009**, *3*, 55–66.
2. Alaci, D.S.A. Regulating Urbanisation in Sub-Saharan Africa Through Cluster Settlements: Lessons for urban managers in Ethiopia. *Theor. Empir. Res. Urban Manag.* **2019**, *5*, 16.
3. Adebowale, B.I.; Kayode, S.E. Geospatial Assessment of Urban Expansion and Land Surface Temperature in Akure, Nigeria. In Proceedings of the ICUC9—9th International Conference on Urban Climate Jointly with 12th Symposium on the Urban Environment, Toulouse, France, 20–24 July 2015.
4. Satterthwaite, D. Climate change and urbanization: Effects and implications for urban governance. In Proceedings of the United Nations Expert Group Meeting on Population Distribution, Urbanization, Internal Migration and Development, New York, NY, USA, 21–23 January 2008; pp. 21–23.
5. Sayemuzzaman, M.; Jha, M.K. Modeling of Future Land Cover Land Use Change in North Carolina Using Markov Chain and Cellular Automata Model. *Am. J. Eng. Appl. Sci.* **2014**, *7*, 295–306. [[CrossRef](#)]
6. Owoeye, J.O.; Popoola, O.O. Predicting urban sprawl and land use changes in Akure region using markov chains modeling. *J. Geogr. Reg. Plan.* **2017**, *10*, 197–207. [[CrossRef](#)]
7. Müller, N.; Ignatieva, M.; Nilon, C.H.; Werner, P.; Zipperer, W.C. *Patterns and Trends in Urban Biodiversity and Landscape Design*; Springer: Dordrecht, The Netherlands; Heidelberg, Germany; New York, NY, USA; London, UK, 2013; ISBN 978-94-007-7087-4.
8. United Nations World Urbanization Prospects—Population Division—United Nations. Available online: <https://population.un.org/wup/> (accessed on 21 September 2019).
9. Mohan, M.; Pathan, S.K.; Narendrareddy, K.; Kandya, A.; Pandey, S. Dynamics of Urbanization and Its Impact on Land-Use/Land-Cover: A Case Study of Megacity Delhi. *JEP* **2011**, *2*, 1274–1283. [[CrossRef](#)]
10. Yu, D.; Yanxu, L.; Bojie, F. Urban growth simulation guided by ecological constraints in Beijing city: Methods and implications for spatial planning. *J. Environ. Manag.* **2019**, *243*, 402–410. [[CrossRef](#)]
11. UN HABITAT. *State of the World Cities 2010/2011: Bridging the Urban Divide*; Earthscan: London, UK, 2007.
12. Lohnert, B. *Migration and the Rural-Urban Transition in Sub-Saharan Africa*; SLE Discussion Paper; Seminar für ländliche Entwicklung (SLE): Berlin, Germany, 2017; ISBN 978-3-936602-90-6.
13. African Development Bank Organisation for Economic Co-operation and Development. United Nations Development Programme: Part II Sustainable cities and structural transformation. In *African Economic Outlook 2016*; Available online: [https://www.afdb.org/fileadmin/uploads/afdb/Documents/Publications/AEO\\_2016\\_Report\\_Full\\_English.pdf](https://www.afdb.org/fileadmin/uploads/afdb/Documents/Publications/AEO_2016_Report_Full_English.pdf) (accessed on 5 January 2019).
14. Malaviya, S.; Munsli, M.; Oinam, G.; Joshi, P.K. Landscape approach for quantifying land use land cover change (1972–2006) and habitat diversity in a mining area in Central India (Bokaro, Jharkhand). *Environ. Monit. Assess.* **2010**, *170*, 215–229. [[CrossRef](#)]
15. Punia, M.; Singh, L. Entropy Approach for Assessment of Urban Growth: A Case Study of Jaipur, India. *J. Indian Soc. Remote Sens.* **2012**, *40*, 231–244. [[CrossRef](#)]
16. Yuan, F.; Sawaya, K.E.; Loeffelholz, B.C.; Bauer, M.E. Land cover classification and change analysis of the Twin Cities (Minnesota) Metropolitan Area by multitemporal Landsat remote sensing. *Remote Sens. Environ.* **2005**, *98*, 317–328. [[CrossRef](#)]
17. Mundia, C.N.; Aniya, M. Analysis of land use/cover changes and urban expansion of Nairobi city using remote sensing and GIS. *Int. J. Remote Sens.* **2005**, *26*, 2831–2849. [[CrossRef](#)]
18. Hove, M.; Tirimboi, A. Assessment of Harare Water Service Delivery. *J. Sustain. Dev. Afr.* **2011**, *13*, 61–84.
19. Wania, A.; Kemper, T.; Tiede, D.; Zeil, P. Mapping recent built-up area changes in the city of Harare with high resolution satellite imagery. *Appl. Geogr.* **2014**, *46*, 35–44. [[CrossRef](#)]
20. Abdullah, A.Y.M.; Masrur, A.; Adnan, M.S.G.; Baky, M.A.A.; Hassan, Q.K.; Dewan, A. Spatio-temporal Patterns of Land Use/Land Cover Change in the Heterogeneous Coastal Region of Bangladesh between 1990 and 2017. *Remote Sens.* **2019**, *11*, 790. [[CrossRef](#)]
21. As-syakur, A.R.; Adnyana, I.W.S.; Arthana, I.W.; Nuarsa, I.W. Enhanced Built-Up and Bareness Index (EBBI) for Mapping Built-Up and Bare Land in an Urban Area. *Remote Sens.* **2012**, *4*, 2957–2970. [[CrossRef](#)]
22. Noon, I.K.; Duker, A.A.; Van Duren, I.; Addae-Wireko, L.; Osei Jnr, E.M. Support vector machine to map oil palm in a heterogeneous environment. *Int. J. Remote Sens.* **2014**, *35*, 4778–4794. [[CrossRef](#)]



23. Chemura, A.; Mutanga, O. Developing detailed age-specific thematic maps for coffee (*Coffea arabica* L.) in heterogeneous agricultural landscapes using random forests applied on Landsat 8 multispectral sensor. *Geocarto Int.* **2017**, *32*, 759–776. [[CrossRef](#)]
24. Sinha, P.; Verma, N.K.; Ayele, E. Urban Built-up Area Extraction and Change Detection of Adama Municipal Area using Time-Series Landsat Images. *Int. J. Adv. Remote Sens. GIS* **2016**, *5*, 1886–1895. [[CrossRef](#)]
25. Faridatul, M.I.; Wu, B. Automatic Classification of Major Urban Land Covers Based on Novel Spectral Indices. *IJGI* **2018**, *7*, 453. [[CrossRef](#)]
26. Kamusoko, C.; Gamba, J.; Murakami, H. Monitoring Urban Spatial Growth in Harare Metropolitan Province, Zimbabwe. *Adv. Remote Sens.* **2013**, *2*, 322–331. [[CrossRef](#)]
27. Hegazy, I.R.; Kaloop, M.R. Monitoring urban growth and land use change detection with GIS and remote sensing techniques in Daqahlia governorate Egypt. *Int. J. Sustain. Built Environ.* **2015**, *4*, 117–124. [[CrossRef](#)]
28. Chirisa, I.E.W.; Muhomba, K. Constraints to managing urban and housing land in the context of poverty: A case of Epworth settlement in Zimbabwe. *Local Environ.* **2013**, *18*, 950–964. [[CrossRef](#)]
29. Shafizadeh Moghadam, H.; Helbich, M. Spatiotemporal urbanization processes in the megacity of Mumbai, India: A Markov chains-cellular automata urban growth model. *Appl. Geogr.* **2013**, *40*, 140–149. [[CrossRef](#)]
30. Mushore, T.D.; Odindi, J.; Dube, T.; Mutanga, O. Prediction of future urban surface temperatures using medium resolution satellite data in Harare metropolitan city, Zimbabwe. *Build. Environ.* **2017**, *122*, 397–410. [[CrossRef](#)]
31. Tibaijuka, A.K. *Report of the Fact-Finding Mission to Zimbabwe to Assess the Scope and Impact of Operation Murambatsvina*; United Nations: New York, NY, USA, 2005.
32. Potts, D. “We Have A Tiger by the Tail”: Continuities and Discontinuities in Zimbabwean City Planning and Politics. *Crit. Afr. Stud.* **2011**, *4*, 15–46. [[CrossRef](#)]
33. Nyamapfene, K. *Soils of Zimbabwe*; Nehanda Publishers: Harare, Zimbabwe, 1991.
34. Anderson, I.P.; Brinn, P.J.; Moyo, M.; Nyamwanza, B. *Physical Resource Inventory of the Communal Lands of Zimbabwe—An Overview (NRI Bulletin 60)*; Natural Resources Institute: Chatham Maritime, Kent, UK, 1993.
35. Lister, L.A.; Phil, D. *The Erosion Surfaces of Zimbabwe*; Zimbabwe Geological Survey Bulletin, No. 90; Geological Survey Department: Harare, Zimbabwe, 1987.
36. CSO (Central Statistical Office). *Census 2002 Population Census: Provincial Profile Harare*; CSO (Central Statistical Office): Harare, Zimbabwe, 2004.
37. *ZimStats (Zimbabwe National Statistics Agency) Census 2012: Preliminary Report*; Harare, Zimbabwe, 2012; Available online: <http://www.zimstat.co.zw/sites/default/files/img/publications/Population/Harare.pdf> (accessed on 7 August 2018).
38. Patley, M.; Tripathi, R.; Lokesh, P. Urbanization and Change Detection of Land Use Land Cover of the Holy City Ujjain. *Int. J. Sci. Eng. Res.* **2018**, *9*. [[CrossRef](#)]
39. Chander, G.; Markham, B.L.; Helder, D.L. Summary of current radiometric calibration coefficients for Landsat MSS, TM, ETM+, and EO-1 ALI sensors. *Remote Sens. Environ.* **2009**, *113*, 893–903. [[CrossRef](#)]
40. Castillejo-González, I.L.; Pena-Barragán, J.M.; Jurado-Expósito, M.; Mesas-Carrascosa, F.J.; López-Granados, F. Evaluation of pixel-and object-based approaches for mapping wild oat (*Avena sterilis*) weed patches in wheat fields using QuickBird imagery for site-specific management. *Eur. J. Agron.* **2014**, *59*, 57–66. [[CrossRef](#)]
41. Mwakapuja, F.; Liwa, E.; Kashaigili, J. Usage of Indices for Extraction of Built-up Areas and Vegetation Features from Landsat TM Image: A Case of Dar Es Salaam and Kisarawe Peri-Urban Areas, Tanzania. *Int. J. Agric. For.* **2013**, *3*, 273–283.
42. Vapnik, V.N. *The Nature of Statistical Learning Theory*; John Wiley & Sons: New York, NY, USA, 1998.
43. Congalton, R.G. A review of assessing the accuracy of classifications of remotely sensed data. *Remote Sens. Environ.* **1991**, *37*, 35–46. [[CrossRef](#)]
44. Xu, H. Modification of normalised difference water index (NDWI) to enhance open water features in remotely sensed imagery. *Int. J. Remote Sens.* **2006**, *27*, 3025–3033. [[CrossRef](#)]
45. Huete, A.R. A soil-adjusted vegetation index (SAVI). *Remote Sens. Environ.* **1988**, *25*, 295–309. [[CrossRef](#)]
46. Anselm, N.; Brokamp, G.; Schütt, B. Assessment of Land Cover Change in Peri-Urban High Andean Environments South of Bogotá, Colombia. *Land* **2018**, *7*, 75. [[CrossRef](#)]
47. Herron, M.C. Postestimation Uncertainty in Limited Dependent Variable Models. *Polit. Anal.* **1999**, *8*, 83–98. [[CrossRef](#)]

48. Pontius, R.G.; Schneider, L.C. Land-cover change model validation by an ROC method for the Ipswich watershed, Massachusetts, USA. *Agric. Ecosyst. Environ.* **2001**, *85*, 239–248. [[CrossRef](#)]
49. Pontius, R.G., Jr.; Batchu, K. Using the relative operating characteristic to quantify certainty in prediction of location of land cover change in India. *Trans. GIS* **2003**, *7*, 467–484. [[CrossRef](#)]
50. Schubert, H.; Caballero Calvo, A.; Rauchecker, M.; Rojas-Zamora, O.; Brokamp, G.; Schütt, B. Assessment of Land Cover Changes in the Hinterland of Barranquilla (Colombia) Using Landsat Imagery and Logistic Regression. *Land* **2018**, *7*, 152. [[CrossRef](#)]
51. Zhang, H.; Qi, Z.; Ye, X.; Cai, Y.; Ma, W.; Chen, M. Analysis of land use/land cover change, population shift, and their effects on spatiotemporal patterns of urban heat islands in metropolitan Shanghai, China. *Appl. Geogr.* **2013**, *44*, 121–133. [[CrossRef](#)]
52. Herold, M.; Roberts, D.A.; Gardner, M.E.; Dennison, P.E. Spectrometry for urban area remote sensing—Development and analysis of a spectral library from 350 to 2400 nm. *Remote Sens. Environ.* **2004**, *91*, 304–319. [[CrossRef](#)]
53. Kucsicsa, G.; Grigorescu, I. Urban Growth in the Bucharest Metropolitan Area: Spatial and Temporal Assessment Using Logistic Regression. *J. Urban Plan. Dev.* **2018**, *144*, 5017013. [[CrossRef](#)]
54. Cumming, S.D.; Tevera, D.S.; Zinyama, L.M. *Harare: The Growth and Problems of the City*; University of Zimbabwe Publications: Harare, Zimbabwe, 1993.
55. Zinyama, L. The evolution of spatial structure in greater Harare. In *Harare: The Growth and Problems of the City*; Zinyama, L.M., Tevera, D.S., Cumming, D., Eds.; University of Zimbabwe Publications: Harare, Zimbabwe, 1995.
56. Araya, Y.H.; Cabral, P. Analysis and Modeling of Urban Land Cover Change in Setúbal and Sesimbra, Portugal. *Remote Sens.* **2010**, *2*, 1549–1563. [[CrossRef](#)]
57. Kamete, A.Y. Cold-hearted, negligent and spineless? Planning, planners and the (r) ejection of “filth” in urban Zimbabwe. *Int. Plan. Stud.* **2007**, *12*, 153–171. [[CrossRef](#)]
58. Toriro, P. *Town Planning in Zimbabwe: History Challenges and the Urban Renewal Operation Murambatsvina and Operation Garikayi*; OSSREA: Harare, Zimbabwe, 2007.
59. Chirisa, I. Building and urban planning in Zimbabwe with special reference to Harare: Putting needs, costs and sustainability in focus. *Consilience* **2014**, *11*, 1–26.
60. Douglas, I. *The Urban Environment*; Edward Anorld (Publisher) Ltd.: London, UK, 1983.
61. Turrall, H.; Burke, J.; Faurès, J.M. *Climate Change, Water and Food Security*; Water Reports; FAO: Rome, Italy, 2011.
62. Government of Zimbabwe (GoZ). *Report on Development of Human Settlements in Zimbabwe*; Government of Zimbabwe: Harare, Zimbabwe, 1991.



© 2019 by the authors. Licensee MDPI, Basel, Switzerland. This article is an open access article distributed under the terms and conditions of the Creative Commons Attribution (CC BY) license (<http://creativecommons.org/licenses/by/4.0/>).